METALLURGICAL AND MATERIALS ENGINEERING

University of Pittsburgh
Pittsburgh, Pennsylvania 15261

NASA CR-159616

AN INVESTIGATION OF THE INITIATION STAGE OF HOT CORROSION IN Ni-BASE ALLOYS

Progress Report
on
Grant No. NSG-3214

Prepared for

National Aeronautics and Space Administration

by

T. T. Huang
G. H. Meier
Department of Metallurgical and Materials Engineering
University of Pittsburgh
Pittsburgh, Pennsylvania 15261

March 31, 1979

1.0 Statement of the Problem

Experience with stationary gas turbines has shown that deposits of alkali salts on the hot sections of gas turbines result in accelerated oxidation of blade and vane materials. This phenomenon is called hot corrosion.

One may separate hot corrosion into two steps:

1. The initial reactions or events which lead to breakdown of the protective scale.
2. Subsequent reaction between the alloy and the salt or atmosphere.

The critical step in hot corrosion is the destruction of the normally protective oxide layer which separates the fused salt from the substrate. It appears that prevention of hot corrosion must be attained by the prevention of the initiation stage of the reaction. Therefore, an understanding of those processes leading to initiation of hot corrosion should indicate methods of preventing or minimizing alloy degradation.

2.0 Experimental Approach

2.1 Objective

The objective of this program is to study the mechanisms, which lead to the destruction of a normally protective scale during the initial stages of hot corrosion of a series of nickel-base alloys contaminated with Na_2SO_4 and other condensed deposits.

2.2 Experimental

The alloys studied include the commercial Ni-base alloys IN-738 and B-1900. High purity laboratory alloys were prepared to simulate the effects of the major elements in the commercial alloys. The compositions of these alloys are:

Ni-16Cr-3.4Ti

Ni-16Cr-3.4Al

Ni-16Cr-3.4Al-3.4Ti

Ni-16Cr-3.4Al-1.7Mo

Ni-16Cr-3.4Al-2.6

Ni-16Cr-3.4Al-1.7Ta

Ni-16Cr-3.4Al-1.7Mo-2.6W

Ni-16Cr-3.4Al-3.4Ti-1.7Mo

Ni-16Cr-3.4Al-3.4Ti-2.6W

Ni-16Cr-3.4Al-3.4Ti-2.6W-1.7Mo

Ni-16Cr-3.4Al-3.4Ti-1.7Ta

Ni-16Cr-3.4Al-3.4Ti-1.7Mo-2.6W-1.7Ta

and

Ni-16Cr-3.4Al-3.4Ti-1.7Mo-2.6W-1.7Ta-0.17C

Ni-16Cr-3.4Al-3.4Ti-1.7Mo-2.6W-1.7Ta-8.5Co-1.0Cb-0.17C

The laboratory alloys were tungsten arc melted under an argon atmosphere, remelted several times, and drop-cast into a water cooled copper chill. The alloys were homogenized for 72 hours in evacuated quartz capsules at 1050°C. The commercial alloy IN-738 was supplied by INCO as 23/4 inch diameter bar in the as-vacuum-cast condition.

Alloy B-1900 (no Hf) and B-1900 (Hf) were supplied by NASA Lewis in sheet form. The commercial alloys were given conventional heat treatments for the individual alloys. Specimen coupons were cut from the alloys, polished through 600 grit silicon carbide and cleaned ultrasonically. The salt coatings were applied by spraying with their aqueous solutions while the coupons were heated using a hot plate and a heat lamp. Coating weights were generally 1 mg/cm^2. A limited number of specimens were coated with heavier salt deposits.

A continuous reading Cahn microbalance was used to record weight changes at temperatures between 900^o and 1000^{o}C at 1 atmosphere pressure of slowly flowing oxygen. The reaction was initiated by raising a preheated furnace around the quartz furnace tube in which the specimen was supported with oxygen flowing. The furnace was raised in a time period of ten seconds. At 900^{o}C the system and specimen came to thermal equilibrium in less than one minute. Oxidized specimens were studied using optical and scanning electron metallography and x-ray diffraction techniques. Transmission electron microscopy and electron diffraction have also been used to identify the structure of carbides in some commercial alloys.

3.0 Experimental Results and Discussion

3.1 IN-738

Curve B in Figure 1 shows the rate of simple oxidation of IN-738 at 977^{o}C. The rate which is approximately parabolic is determined by the formation of a thin external scale containing Cr_2O_3 and TiO_2 (Figure 2). The needle-like internal precipitates are Al_2O_3 and the

large white particles are carbides, which are reported by R. A. Stevens and P. E. J. Flewitt[1] to be $(Ti_{0.50}, Ta_{0.20}, Nb_{0.20}, W_{0.40}, Cr_{0.02}, Zr_{0.01})C$, although our EDAX results show a different composition of these carbides. A corresponding transmission electron micrograph and diffraction pattern of these carbides are shown in Figure 3(a) and 3(b), which shows a fcc structure of mean lattice parameter 0.450 nm. This structure and value for the lattice parameter is consistent with an MC-type carbide[2,3].

Figure 4 shows the rate of oxidation of IN-738 at 900°C when coated with 1 mg/cm^2 of salt indicating the presence of the salts does not appreciably affect the oxidation rate for times up to 190 hours. The morphology of the scale shown in Figure 5 is essentially the same as that observed for simple oxidation at this temperature except for the presence of (Cr, Ti) sulfides formed by sulfur from the salts having penetrated the TiO_2 and Cr_2O_3 scale.

The effect of the salt on the oxidation of IN-738 becomes significant at temperatures greater than 900°C, even for short times. Figure 6 shows the effect of temperature on the oxidation rate of Na_2SO_4-coated IN-738. It is seen that the curve is characteristic of three stages. Stage I is an incubation period, which is characterized by a slow oxidation rate, Stage II is a period of accelerated oxidation during which the rate is slightly increased, and Stage III is a breakaway period, during which a linear oxidation rate obtains. It is clear the curves are temperature sensitive. In Figure 7 the time to breakaway (τ), which is arbitrarily chosen as the time to reach a weight change of 10 mg/cm^2, is shown as a function of temperature. The time to breakaway is a minimum at approximately 970°C.

In order to study the hot corrosion characteristics of IN-738 and hopefully describe its temperature dependence, a series of specimens were subjected to hot corrosion at 950°C with the reaction being interrupted at different stages. The results of optical and scanning electron metallography are as follows.

Stage I:

Figure 8(a) shows the scale on a specimen coated with Na_2SO_4 and oxidized at 950°C for 1 hour. It is clear the scale was broken down locally allowing the salt to penetrate the scale to the scale/metal interface. Figure 8(b) is an Al EDAX scan of Figure 8(a), showing Al_2O_3 as well as Cr_2O_3 will dissolve into the salt. There are many possible reasons for scale breakdown. It may be due to growth stresses or due to complex chemical attack, for example, fluxing. In order to study the mechanism of scale breakdown, a specimen was polished through 600 grit, coated with Na_2SO_4, and oxidized at 970°C for 10 minutes. The specimen was then dipped into boiled water for 10 minutes to wash away the remaining salts, and the surface was examined under S.E.M., Figure 9 shows the as-polished surface and Figure 10 the oxidized surface. It is evident the scale is broken down at regions A, B, and C of Figure 10(a). Figure 10(b) is a higher magnification of area A. EDAX results suggest this region may be the place where carbides were originally present on the surface. Figure 8(c) is a higher magnification of Figure 8(a), and Figure 8(b) is the Ti-scan showing the Ti distribution corresponding to 8(c). The Ti is concentrated around the crack, suggesting the Ti-rich carbide may be dissolved into the salt, resulting in a localized shift

to produce a more acidic salt. One can also see some remaining carbides around the cracks at regions A and B. Localized breakdown could then occur by acid fluxing. If this is the case, then one would expect a preoxidized specimen, with a thicker continuous scale to delay the breakdown of the scale. Figure 11 shows the oxidation curve of IN-738, which was preoxidized at 900°C for 1 hour, cooled to room temperature, sprayed with 1 mg/cm^2 Na_2SO_4 and then subjected to hot corrosion at 970°C. It is clear the incubation times are extended greatly. Figure 12(a) shows the specimen after preoxidation at 900°C for 1 hour. A continuous $NiCr_2O_4$ scale has formed. The white particles are carbides. Figure 12(b) shows, the preoxidized specimen which was coated with Na_2SO_4, and oxidized at 970°C for 1 hour. Apparently the surface carbides have begun to dissolve. Figure 13 shows the scale on a Na_2SO_4-coated specimen, oxidized at 950°C for 6 hours. A layered Cr_2O_3-rich scale indicates the repetitive penetration of salt through a localized region to the scale/metal interface. Figures 14(a) and (b), are the scale and a corresponding Na x-ray map of a specimen, subjected to hot corrosion at 977°C for 8 hours. The salt is present at the scale/metal interface.

Stage II:

Figures 15(a) and (b) show the scale on IN-738, which was coated with Na_2SO_4 and oxidized at 950°C for 10 hours. At this stage the sulfur potential in the salt increases since the sulfate is present at the scale/metal interface where the oxygen potential is smaller than at the scale/gas interface. This results in extensive formation of sulfides,

(Cr, Ti)S, which tie up a large amount of Cr and Ti making it difficult for a protective scale to reform.

Stage III:

Figure 16 shows the scale on IN-738 which has been exposed for 8 hours with a 1 mg/cm^2 coating of pure Na_2SO_4 and which has started to undergo breakaway attack at the specimen corner. The sequence of micrographs in Figure 16(a-c) shows the scale morphology at locations chosen near the specimen center and moving toward the corner. Figure 16(a) taken from the specimen center where the scale is protective, is essentially the same as that for simple oxidation except for the presence of internal sulfides below the zone of internal oxidation. Figure 16(b) is a site chosen closer to the corner showing the start of scale breakdown. The internal sulfides are becoming more massive and in the region to the right of the micrograph where the scale is bulging there is an absence of internal Al_2O_3 particles with the Al being incorporated into the scale. Figure (c) shows the scale/metal interface near the specimen corner where breakaway has begun. The scale, not shown, is greater than 70μm thick. The formation of sulfides along the grain boundaries lifts portions of the alloy into the scale. These are subsequently oxidized to form a layered NiO scale.

For further confirmation of the role of carbides in the initiation of hot corrosion, a portion of the IN-738 ingot received from INCO was remelted in an argon atmosphere, and drop-cast into a water cooled copper chill, with dimensions 1" x 3/8" x 6". This process produced an alloy with smaller carbides. Figure 17(a) and (b)

show the difference in carbide size before and after remelting. Sepcimens cut from the remelted IN-738 were coated with Na_2SO_4 and $Na_2SO_4 + K_2SO_4$ (20%) and subjected to hot corrosion at 970°C. The rate curves are also shown in Figure 11. It is obvious the reduction in carbide size has a great effect on the initiation of hot corrosion in IN-738. Furthermore, a series of remelted IN-738 specimen were subjected to hot corrosion, and interrupted at different times. Figures 18(a-c) show the scale morphology at different stages. Figure 18(a) shows a specimen coated with Na_2SO_4(1 mg/cm^2) and oxidized at 970°C for 1 hour. A very compact scale has formed. The outer regions are mainly Cr_2O_3, Al_2O_3 and TiO_2. The inner protions are Cr_2O_3 and Al_2O_3. Sulfur is observed to diffuse through this scale, forming sulfide underneath. Figure 18(b) shows a specimen exposed at 970°C for 18 hours. Here strong internal oxidation has occurred under a compact Cr_2O_3 scale which is overlaid with a layer of TiO_2. A small amount of sulfide is evident below the internal oxidation zone. It is clear that sulfate was not able to penetrate to the scale/metal interface. Figure 18(c) is the specimen coated with $Na_2SO_4 + K_2SO_4$ (1 mg/cm^2), and oxidized at 970°C for 124 hours. This morphology is basically the same as (b), except the outer scale is thicker and the internal oxidation and sulfidation zones are deeper.

In order to study the effect of microstructure on the hot corrosion resistance of alloys, a series of IN-738 specimens cut from the same ingot were subjected to different heat-treatments. These heat-treatments included heating at 1178°C for 2 hours in Ar and water quenching, heating

at 1178°C for 2 hours in Ar and water quenching followed by annealing in vacuum at 840°C for 24 hours. The oxidation rate of these specimens coated with various salt does not appear significantly different from those for as-cast specimens. Importantly the carbide morphology is almost the same in all these specimens.

The effect of salt chemistry on the oxidation rate of IN-738 is also being studied. The approximate values of the sodium oxide activity in Na_2SO_4, Na_2SO_4 + 20% K_2SO_4, and Na_2SO_4 saturated with SiO_2, MoO_3 and TiO_2 obtained from electrochemical measurements[4] and thermochemical calculations are presented in Table 1. Figure 19 shows the kinetic curves of IN-738 at 977°C with various salt coatings on the surface. The effect of K_2SO_4 on shortening the incubation time at this temperature is not clear now, however, it can be seen that increased salt acidity in the order of Na_2SO_4, Na_2SO_4 + SiO_2 and Na_2SO_4 + TiO_2 corresponds to decreased time to breakaway. This suggests the major influence of carbides is in locally modifying the salt compositions, so the scale is penetrated by the salt exposing a chromium depleted alloy which then undergoes catastrophic attack. Figure 20 shows the scale at the beginning of breakaway for IN-738 coated with 1 mg/cm^2 Na_2SO_4 + K_2SO_4. The thin scale on either side of the NiO mound is Cr_2O_3 overlaid with TiO_2 beneath which is a zone virtually depleted of Cr and Ti by scale formation and internal sulfidation. It is seen that the initially protective scale has been penetrated resulting in the profuse formation of NiO and causing the Cr_2O_3-TiO_2 scale to bulge outward.

Based on the above observations, the following mechanism is suggested to describe the initiation of breakaway hot corrosion in Cr_2O_3-forming superalloys such as IN-738. Initially, a transient oxidation product will form, in this case Al_2O_3, associated with a thin layered scale of Cr_2O_3, overlaid with TiO_2. This depletes the underlying alloy of Cr and Ti. The Al_2O_3 will dissolve into the molten salt. The modified salt dissolves the surface carbides at local regions which increases the Mo, Ti and W content of the salt in this region. The activity of Na_2O in reagent-grade Na_2SO_4 has been approximated at 10^{-12} (see Table 1) which corresponds to a salt in which the solubility of Cr_2O_3 is quite low. This is shown in Figure 21 where the solubility data of Stroud and Rapp[5] are plotted versus a_{Na_2O}. The sodium oxide activities from Table 1 are included as vertical lines. It can be seen that the increased acidity produced by dissolution of Mo, Ti and W-rich carbides into the salt will locally increase the solubility of Cr_2O_3 in the salt and local dissolution of the scale will allow the molten salt to penetrate beneath it and come in contact with a Cr,Ti depleted Ni substrate. Here the P_{O_2} is considerably reduced, so intense sulfidation occurs followed by oxidation of the sulfides and sulfur penetration deeper into the matrix. This cycle continues until the whole specimen is consumed.

A series of alloys have been melted to simulate the effect of the major components of IN-738 on the breakaway behavior. The compositions studied are:

Ni-16Cr-3.4Ti

Ni-16Cr-3.4Al

Ni-16Cr-3.4Al-3.4Ti

Ni-16Cr-3.4Al-1.7Mo

Ni-16Cr-3.4Al-2.6W

Ni-16Cr-3.4Al-1.7Ta

Ni-16Cr-3.4Al-1.7Mo-2.6W

Ni-16Cr-3.4Al-3.4Ti-1.7Mo

Ni-16Cr-3.4Al-3.4Ti-2.6W

Ni-16Cr-3.4Al-3.4Ti-1.7Ta

Ni-16Cr-3.4Al-3.4Ti-1.7Mo-2.6W

Ni-16Cr-3.4Al-3.4Ti-1.7Mo-2.6W-1.7Ta

The behavior of a number of these alloys in simple oxidation is also included in Figure 1. Interestingly none of these alloys undergo breakaway under conditions which produced breakaway in IN-738. The major microstructural feature absent in these alloys is again the complex carbide phase. To further study the effect of carbides the alloy Ni-16Cr-3.4Al-3.4Ti-1.7Mo-2.6W-1.7Ta was carburized for 24 and 48 hours at 1050°C in a graphite pack to produce internal carbides in the surface regions of the alloy. The specimen surfaces were lightly polished to remove surface carbon and carbides and the alloy was exposed in the manner described previously. Figure 22 shows the rate of oxidation of these alloys at 950°C with a 1 mg/cm^2 coating of Na_2SO_4. It is clear, again, that the presence of the carbides has resulted in breakaway corrosion of the carburized alloy while the carbon-free alloy is relatively unaffected by the salt. The carbide morphology in the carburized alloy is not the same as in IN-738 but it is clear that the

carbides are intimately related to the local breakdown of the protective scale. Furthermore, two additional model alloys:

C#13: Ni-16Cr-3.4Al-3.4Ti-1.7Mo-2.6W-1.7Ta-0.17C

C#14: Ni-16Cr-3.4Al-3.4Ti-1.7Mo-2.6W-1.7Ta-8.5Co-1.0Cb-0.17C

have also been prepared. The microstructure of these alloys is shown in Figures 23(a) and (b) and their hot corrosion rates are included in Figure 11. The kinetic results are consistent with the small carbide size in these alloys.

3.2 B-1900

The effect of salt composition on the hot corrosion of alloy B-1900 and B-1900 (with Hf) is also being studied. Figure 24 shows the rate of oxidation of B-1900 at 950°C with several salt coatings. Coating with 1 mg/cm^2 Na_2SO_4 + K_2SO_4 results in a sudden increase in reaction rate at the initial stage. Increasing the acidity of the salt by adding SiO_2 and TiO_2 decreases this initial oxidation rate. The addition of 20 wt% SiO_2 to the salt results in a short incubation period followed by rapid oxidation with the rate approximately equal to that for Na_2SO_4. The specimen coated with Na_2SO_4 + TiO_2 showed a considerably longer incubation time. Apparently, increased acidity of the deposited salt results in the increase in the incubation period of breakaway of B-1900. This is believed due to the prevention of basic fluxing of the transient oxides during the initial stages of exposure.

Figure 25 shows the oxidation behavior of B-1900 and B-1900 (with Hf) coated with Na_2SO_4(1 mg/cm^2). These results show the effect of the

Hf addition is insignificant, and preoxidized specimens do not result in a significant increase in hot corrosion resistance.

Figure 26 shows the scale morphology of B-1900 coated with Na_2SO_4 oxidized at 950°C for 10 hours. The outer layer is mainly NiO and $NiMoO_4$. Intense internal oxidation to form Cr_2O_3 and Al_2O_3 is observed with spherical (Cr,Ni) sulfides present below the internal oxides. Again a layered scale is evident.

4.0 Conclusions

1. The oxidation rate of Na_2SO_4-coated IN-738 between 900 and and 1000°C shows an incubation period which is strongly dependent on temperature and salt composition, followed by rapid breakaway corrosion which begins at specific sites and then spreads over the alloy surface.
2. The breakaway corrosion of IN-738 has been shown to be associated with the presence of carbides in the alloy whose effect has been explained in terms of local modifications in the salt composition.
3. Alloy B-1900 shows rapid corrosion when coated with Na_2SO_4 and $Na_2SO_4 + K_2SO_4$, with essentially no incubation time, while coating with more acidic salts results in a short incubation period prior to breakaway. This indicates a basic fluxing mechanism during the initial exposure period of this alloy.
4. The addition of Hf into B-1900 does not improve the hot corrosion resistance of this alloy.

5.0 Future Plan

1. The effect of alloy elements in IN-738 will be carefully evaluated. The hot corrosion behavior of the model alloys will be examined more closely.
2. The effect of carbides in Ni-base alloys such as IN-738 will be studied more closely. Previous results show, both the salt chemistry and carbide size have significant effects in inducing breakaway type oxidation. In other words, we believe changing the carbide composition and size will also have significant effects on changing the hot corrosion behavior in some of the nickel-base alloys. Further understanding of these factors will provide us a guideline for improved hot corrosion resistance of these alloys without changing other properties significantly. These efforts will include:
   a. Some model alloys with different carbide composition will be prepared and their hot corrosion behavior will be studied.
   b. The carbide morphology in these model alloys will be changed by different heat-treatments in order to study the effect of carbide structure and morphology.
   c. Those elements which can act as a carbide refiner, such as Cb or Hf will be added into those model alloys to study their effects.

REFERENCES

1. R. A. Steven and P. E. J. Flewitt, "The Microstructural Changes which Occur During Isochronal Heat Treatment of the Nickel-Base Superalloy IN-738," Journal of Materials Science, 13, 367, (1978).

2. H. E. Collins, Met. Tran. 5, 189, (1974).

3. R. F. Decker and C. T. Sims, "The Superalloys," edited by C. T. Sims and W. C. Hagel, (Interscience, 1972), p. 73.

4. J. Hines, T. T. Huang, R. A. Stoehr, and G. H. Meier, to be submitted to Corrosion.

5. W. P. Stroud and R. A. Rapp, "The Solubilities of Cr_2O_3 and α-Al_2O_3 in Fused Na_2SO_3 at 1200°K," pp. 574-594, in High Temperature Metal Halide Chemistry, D. L. Hildenbrand and D. D. Cubiccotti, eds., The Electrochem. Soc., (1978).

Table I

Activity of Na_2O in Na_2SO_4 at 1200°K

Salt	Log a_{Na_2O}
Na_2SO_4	-12.1
Na_2SO_4 + 20 mol pct K_2SO_4	-11.6
Na_2SO_4 + SiO_2	-13.1
Na_2SO_4 + MoO_3	-13.9
Na_2SO_4 + TiO_2	-15.7

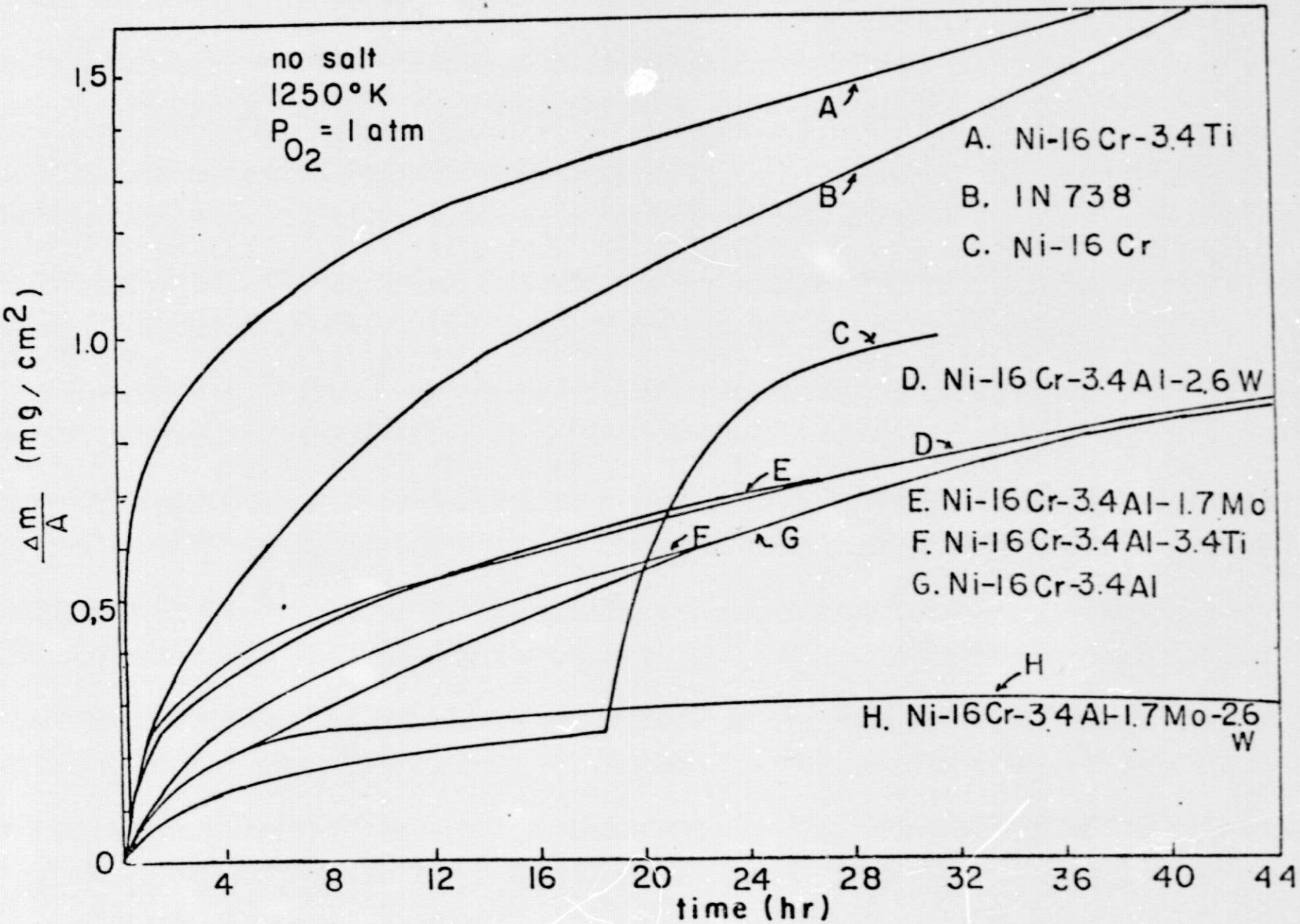

Figure 1 Weight Change vs Time for Ni-base Alloys in Simple Oxidation at 977°C.

Figure 2 IN-738 Oxidized 48 hr at 977°C in 1 atm O_2.

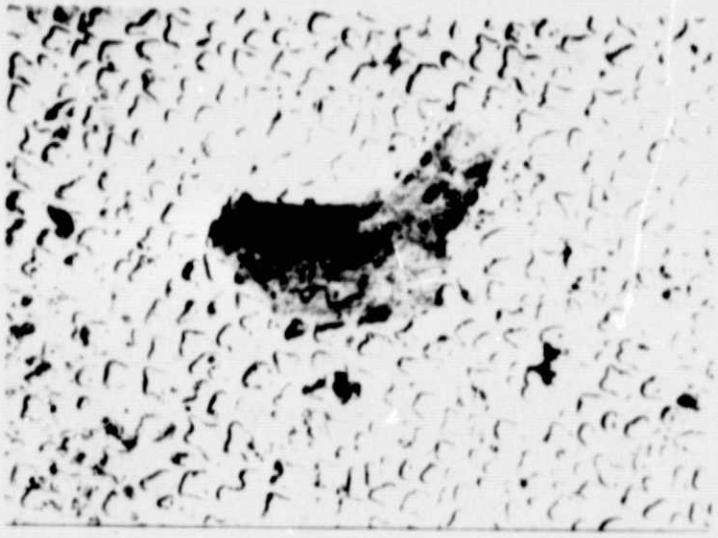

x11000

(a)

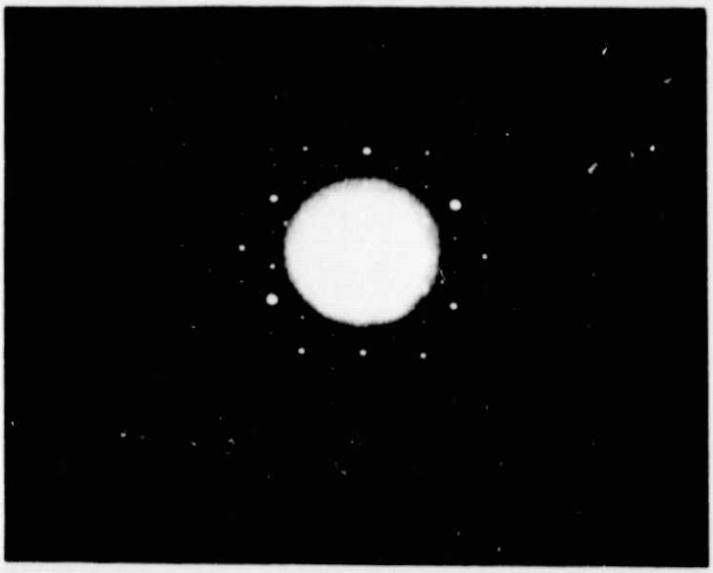

(b)

Figure 3 (a) Transmission electron micrograph of carbide in IN-738, (b) Electron diffraction pattern showing a f.c.c. structure, a = 0.450 nm.

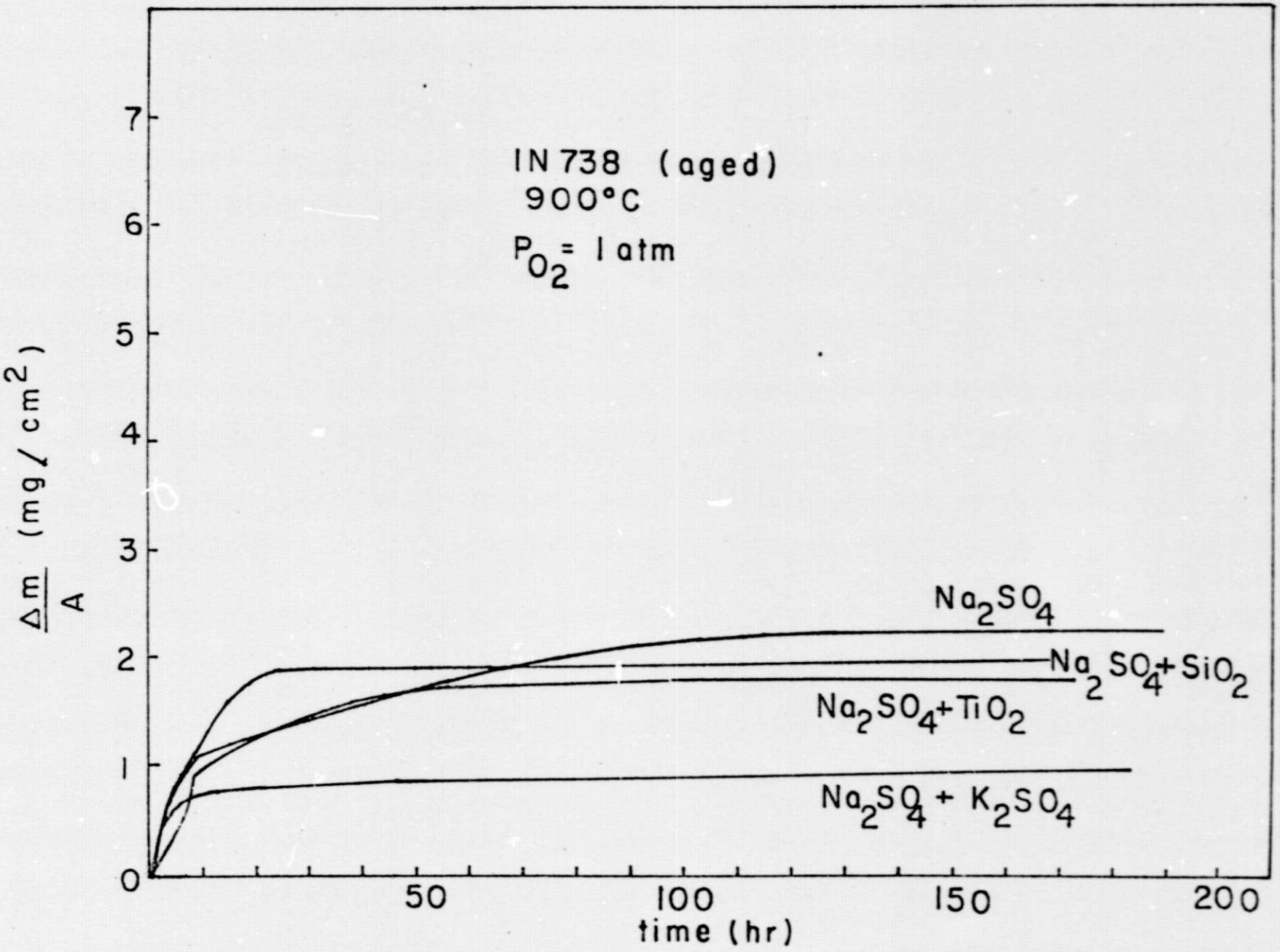

Figure 4 Weight Change vs Time for IN-738 Coated with 1 mg/cm^2 Salt in 1 atm O_2 at 900°C.

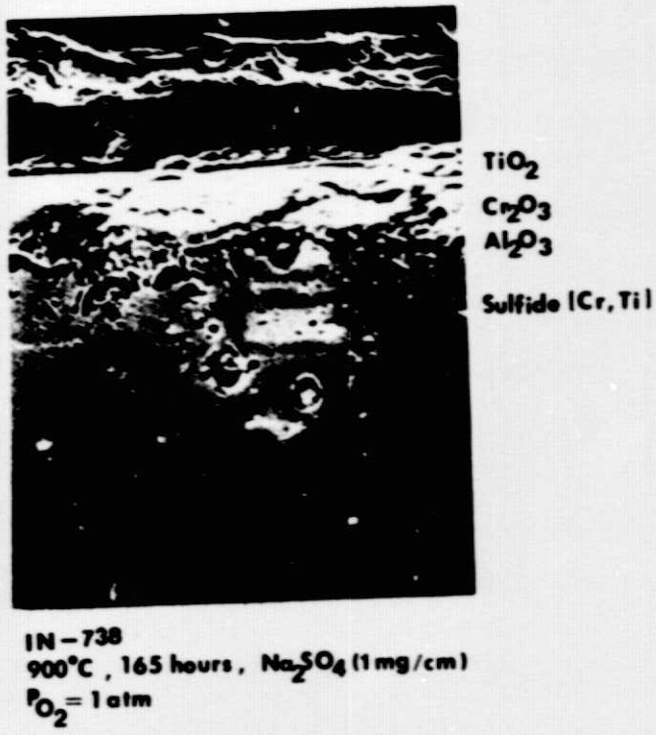

Figure 5 IN-738 Coated with 1 mg/cm^2 Na_2SO_4 and Oxidized 165 hr at 900°C.

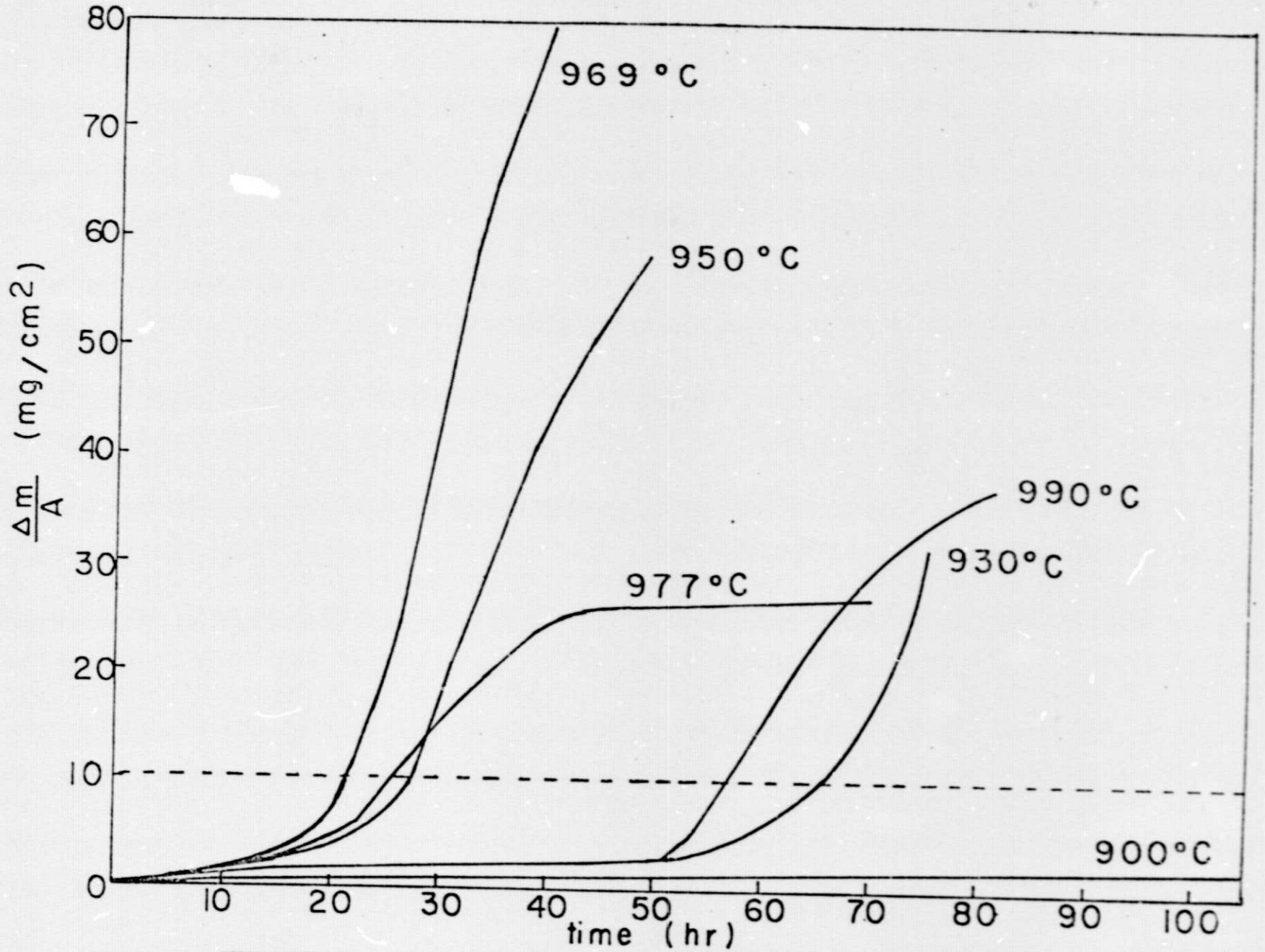

Figure 6 Weight Change vs Time for IN-738 Coated with 1 mg/cm^2 Na_2SO_4 in .1 atm O_2.

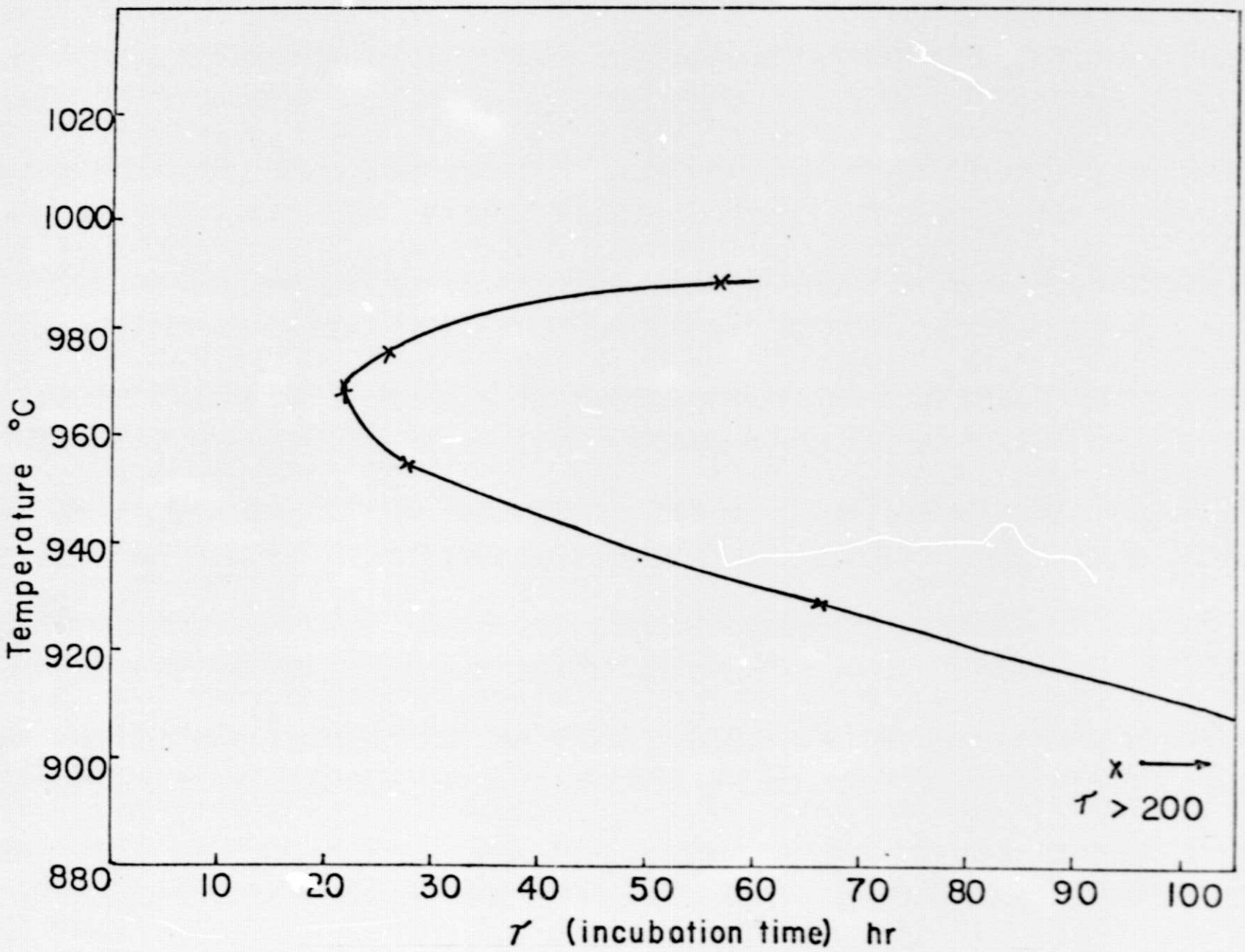

Figure 7 Incubation Time as Function of Temperature for IN-738 Coated with 1 mg/cm^2 Na_2SO_4 in 1 atm O_2.

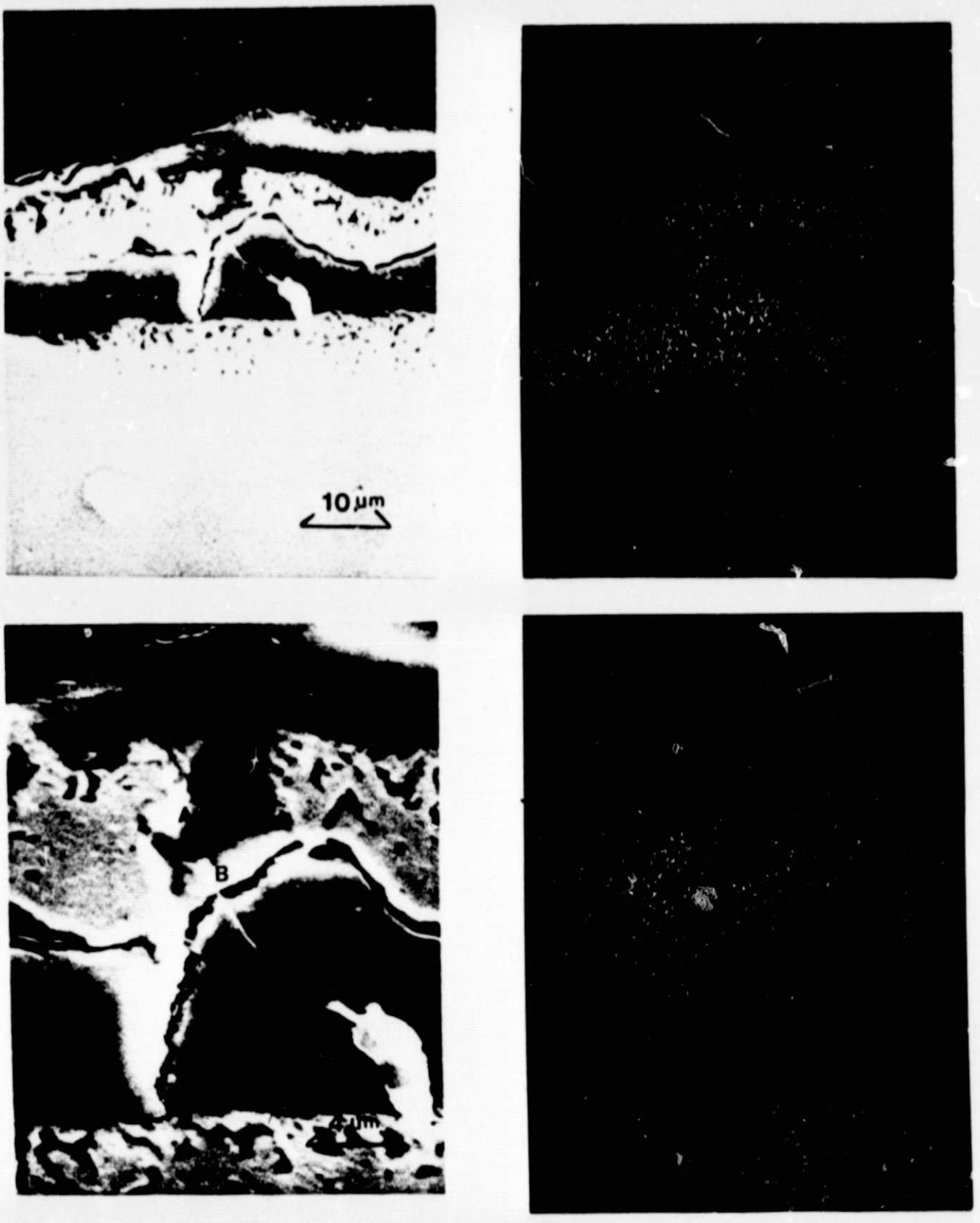

Figure 8 (a) IN-738 Coated with 1 mg/cm2 Na_2SO_4 and Oxidized 1 Hour at 950 C, (b) Al EDAX Scan of (a), (c) A Higher Magnification of (a), (d) Ti EDAX Scan of (c).

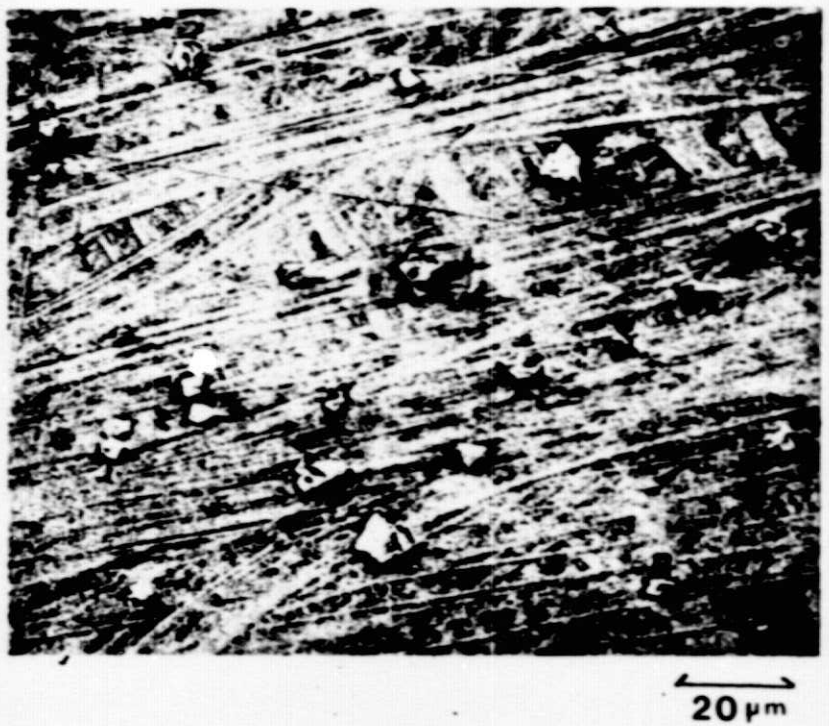

Figure 9 A polished surface of IN-738.

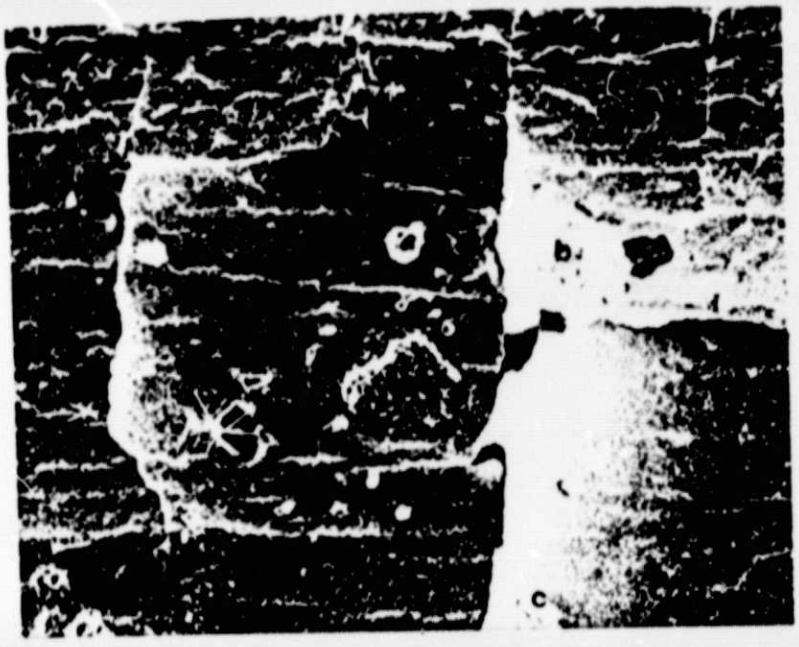

(a) x800

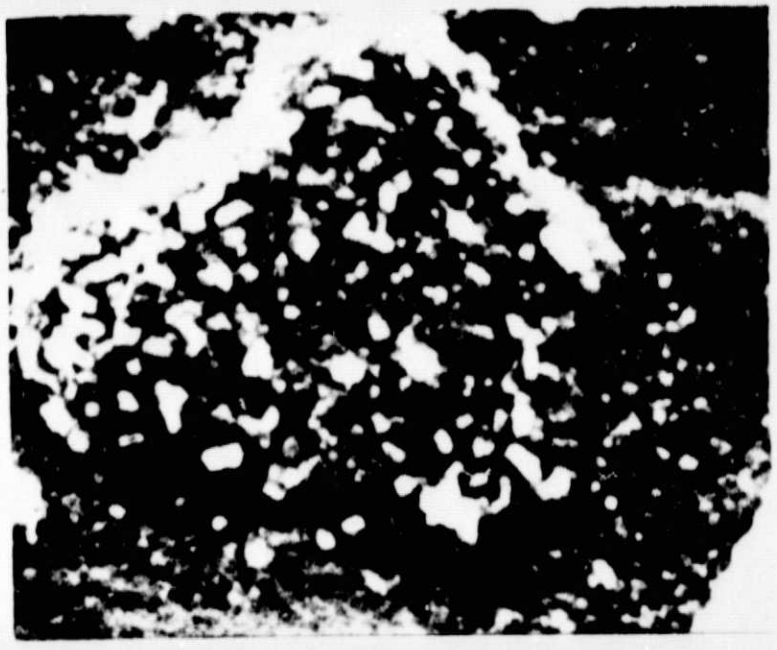

(b) x4000

Figure 10 (a) IN-738 Coated with Na_2SO_4 (1 mg/cm^2), Oxidized at 970 C for 10 minutes, (b) Higher magnification of area a.

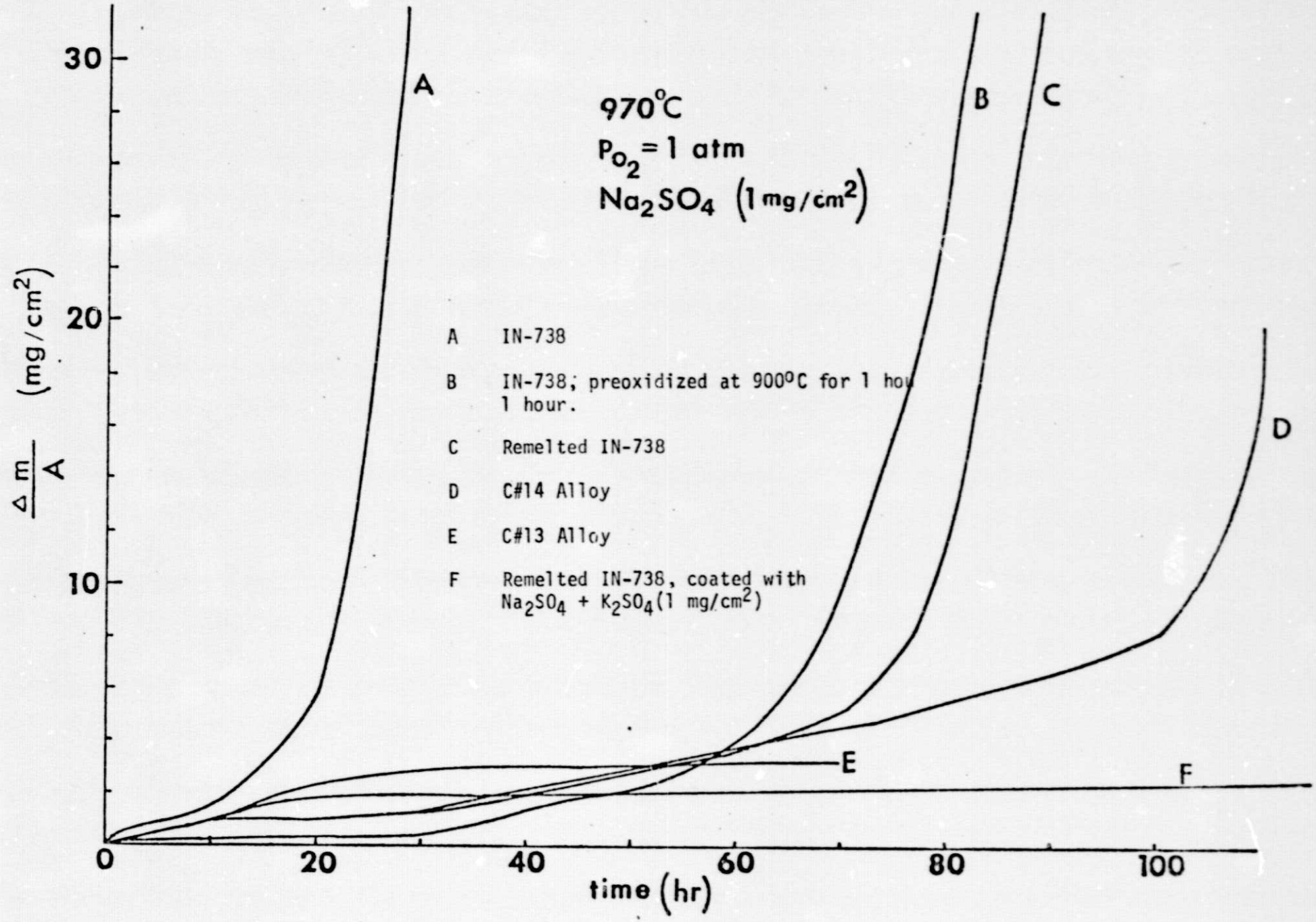

Figure 11 Weight Change vs Time for IN-738 with 1 mg/cm^2 Salt in 1 atm O_2 at 970°C.

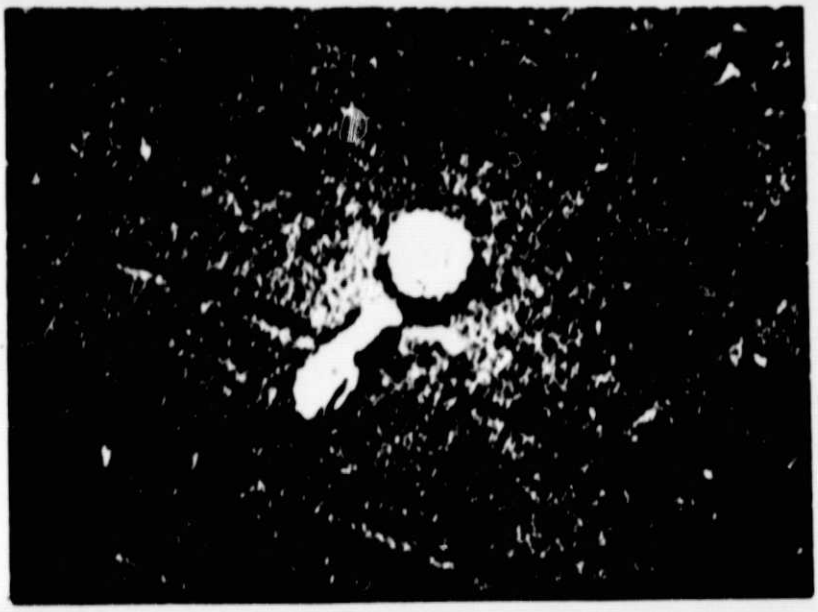

x1600

(a)

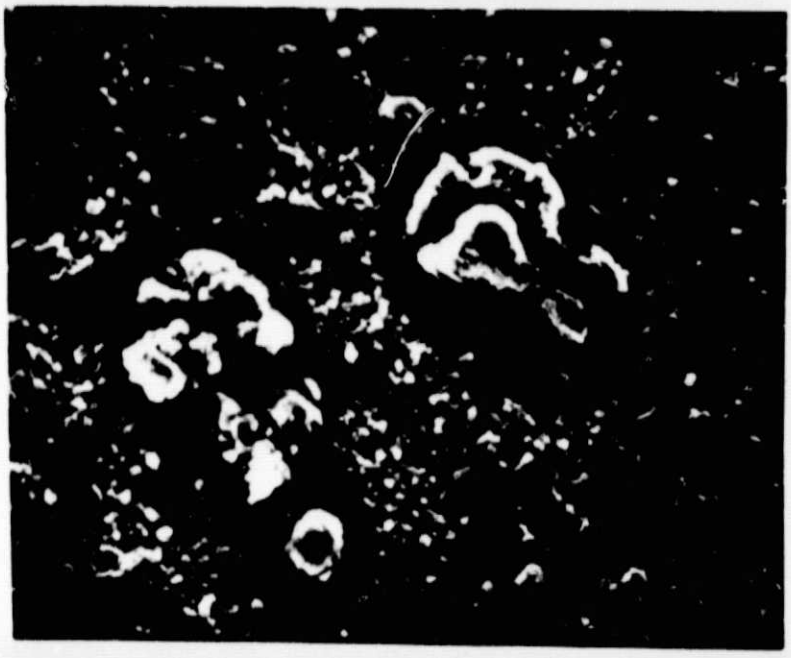

x 4000

(b)

Figure 12 (a) IN-738 preoxidized at 900°C for 1 hour. (b) Preoxidized IN-738, coated with 1 mg/cm^2 Na_2SO_4 and oxidized at 970°C for 1 hour.

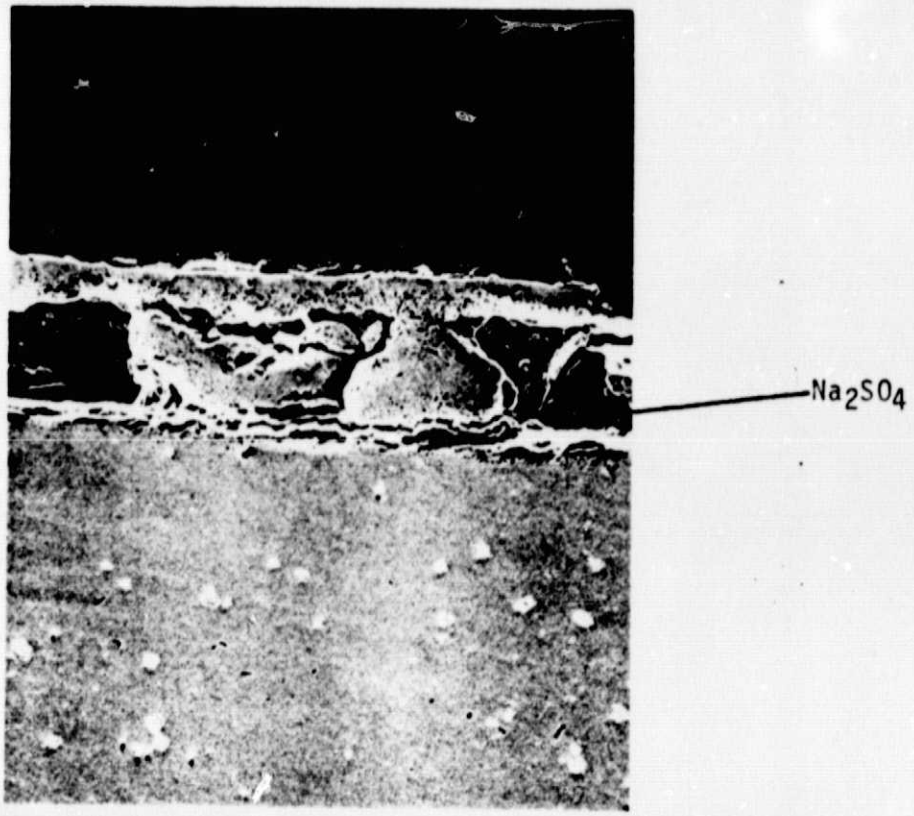

x400

Figure 13 IN-738 coated with 1 mg/cm^2 Na_2SO_4, oxidized at 950°C for 6 hours.

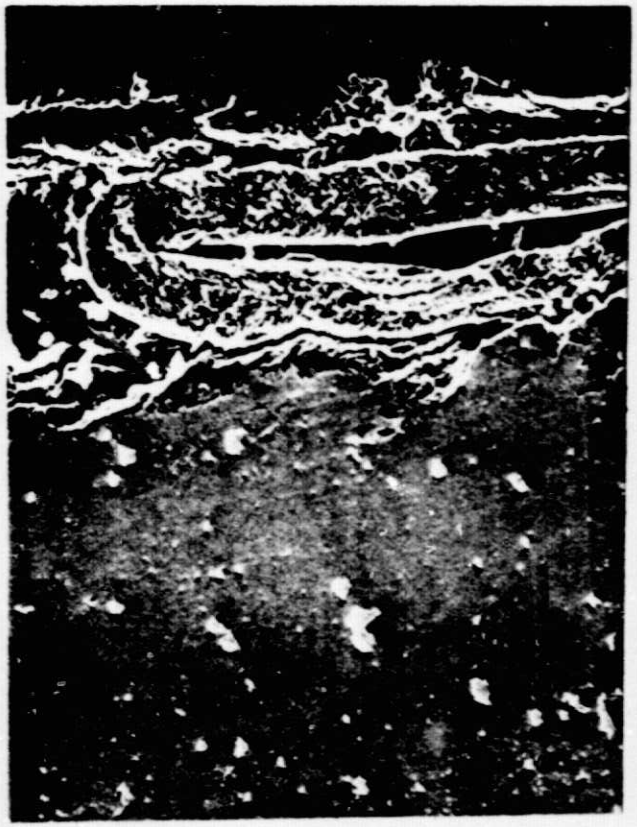

(a)
x400

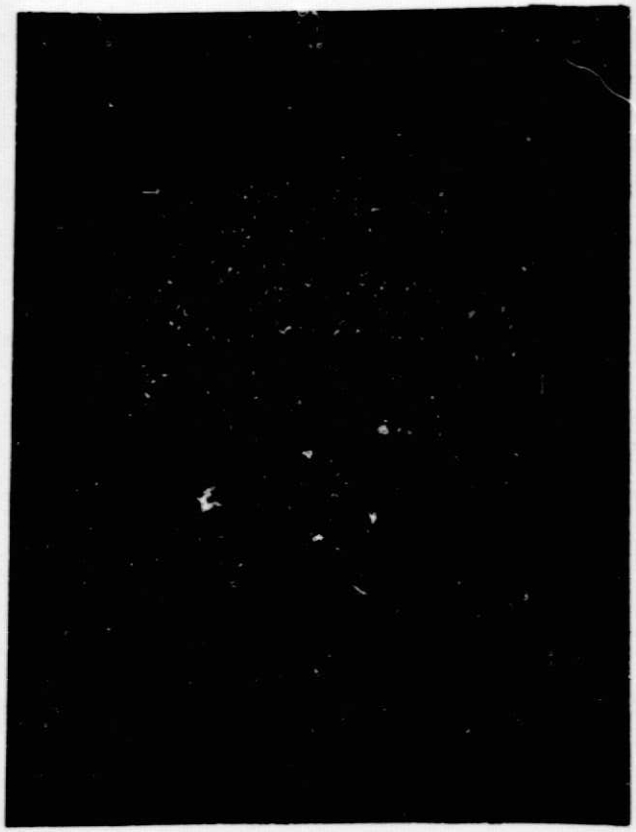

(b)

Figure 14 (a) IN-738 coated with 1 mg/cm^2 Na_2SO_4, oxidized at 977°C for 8 hours, (b) Na x-ray of (a).

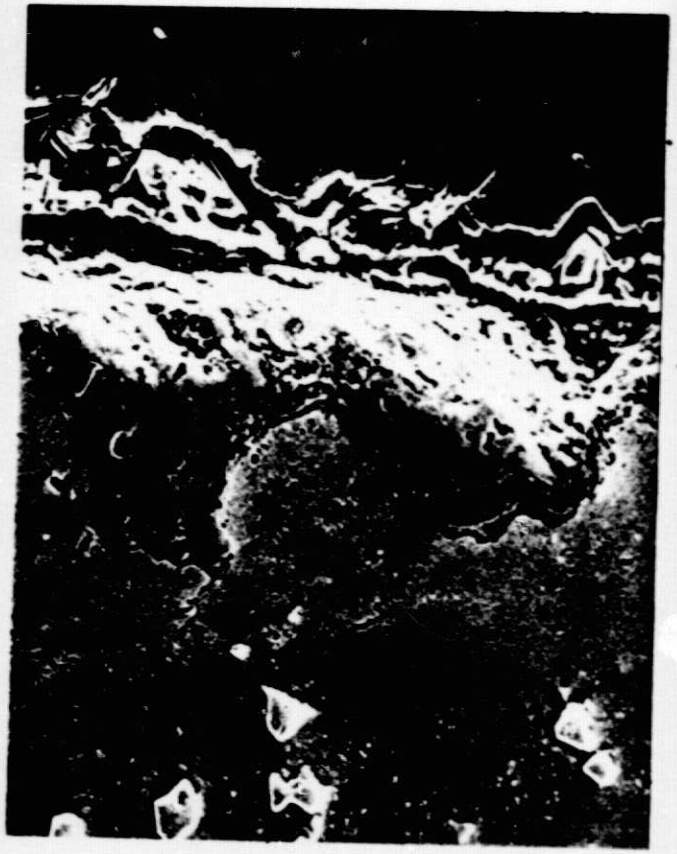

(a)

x800

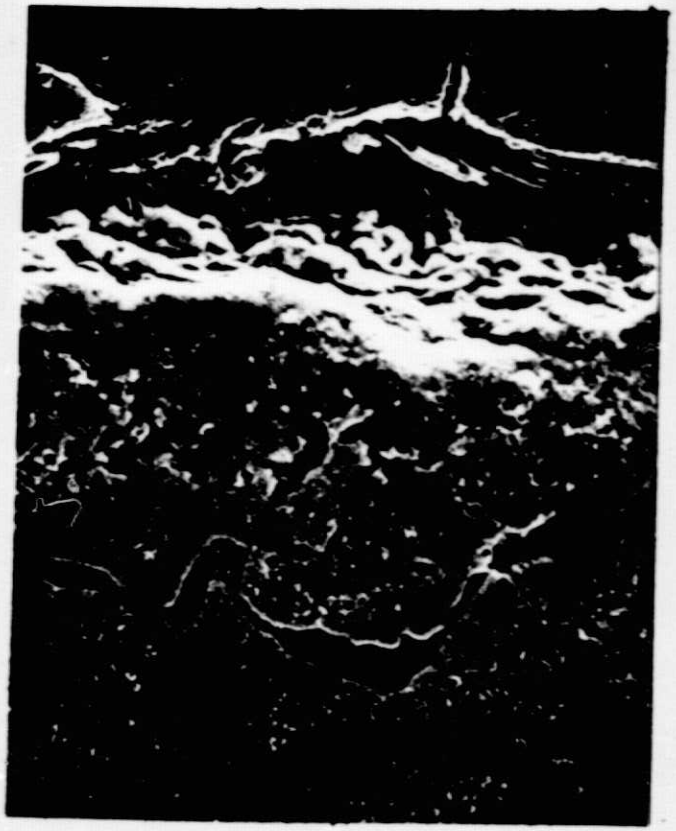

(b)

x800

Figure 15 IN-738, coated with Na_2SO_4 (1 mg/cm2), oxidized at 950°C for 10 hours.

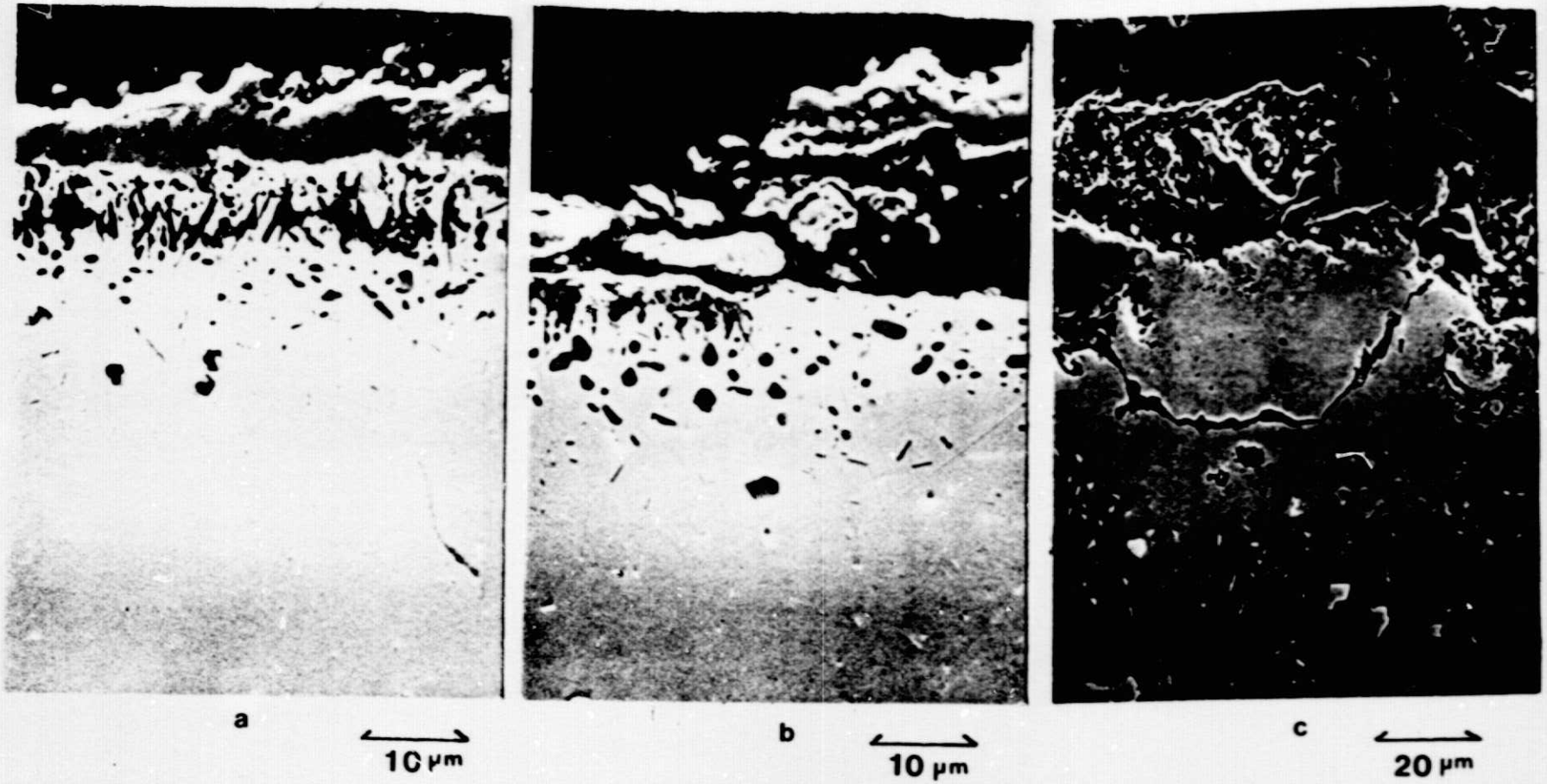

Figure 16 IN-738 Coated with 1 mg/cm^2 Na_2SO_4 and Reacted 8 hr at 977°C in 1 atm O . (a) Specimen Center, (b) Transition Region, (c) Scale Near Corner.

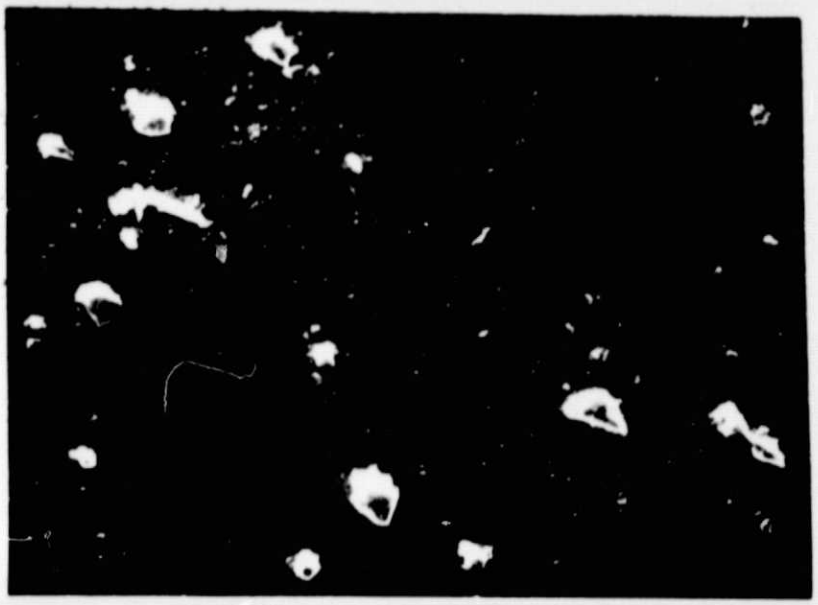

as-received and conventional heat-treated (2152°F 2 hr 840°C 24 hr vacuum)

(a)

20 μm

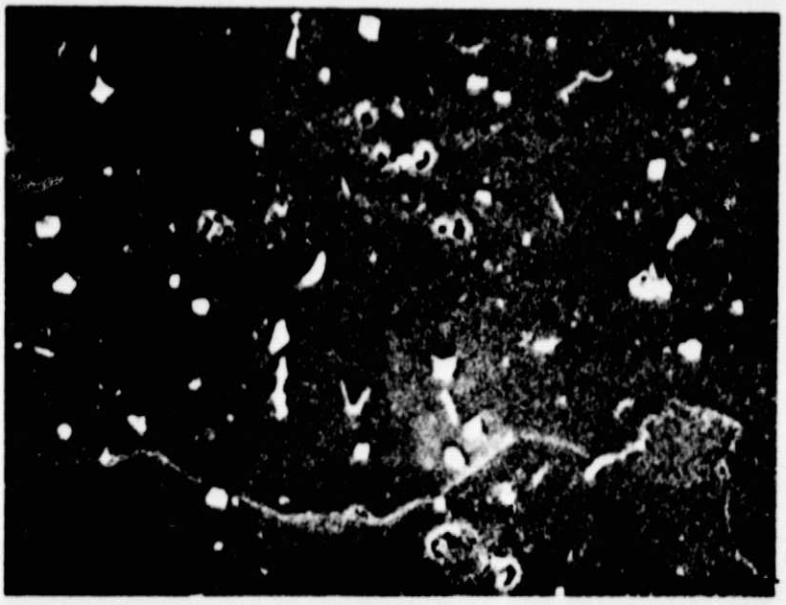

Remelted chill-

(b)

10 μm

Figure 17 (a) IN-738 received from INCO, (b) Remelted IN-738.

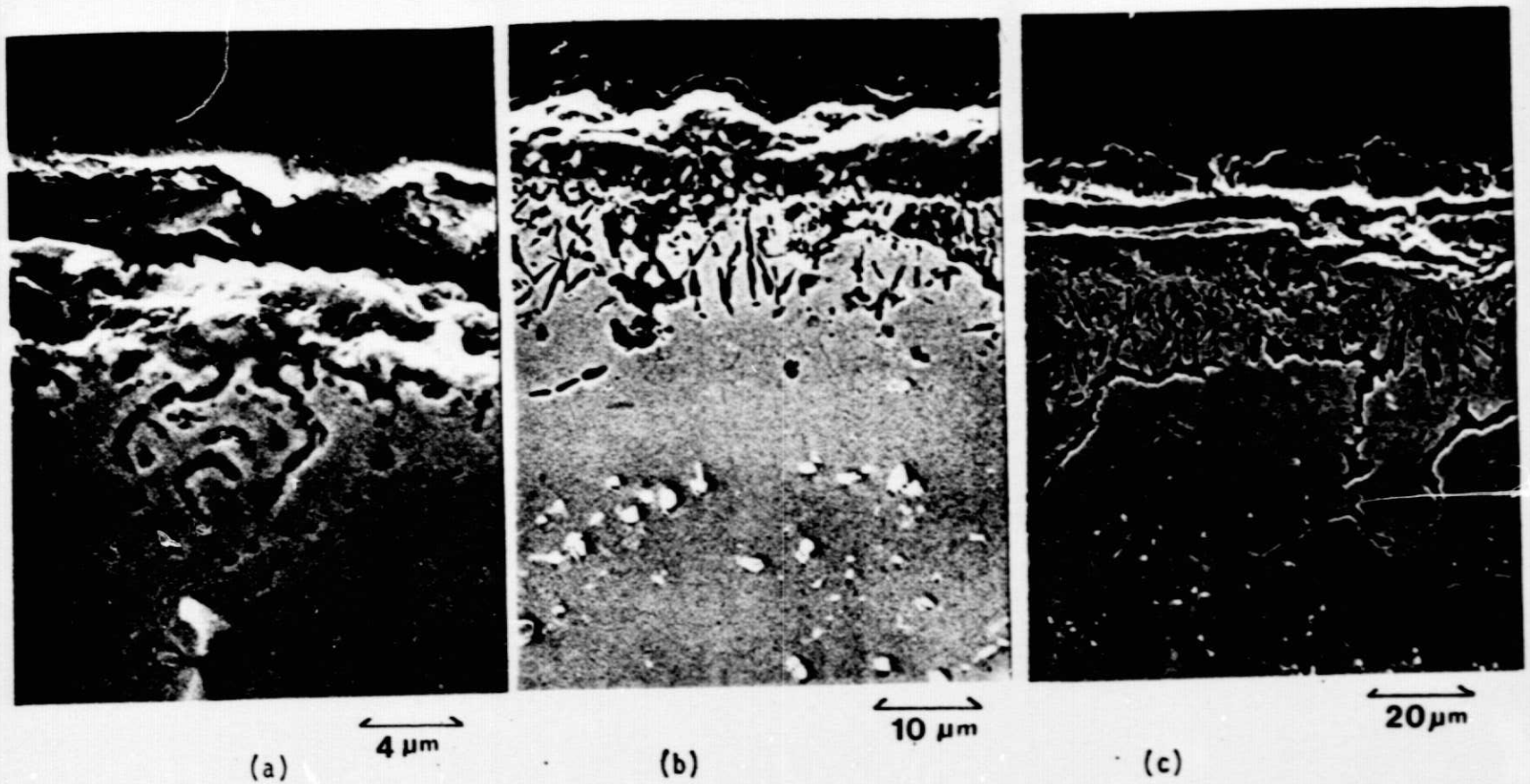

Figure 18 (a) Remelted IN-738 coated with Na_2SO_4 (1 mg/cm^2), oxidized at 970°C for 1 hour, (b) For 18 hours, (c) Remelted IN-738 coated wtih Na_2SO_4 + K_2SO_4 (1 mg/cm^2), oxidized at 970°C for 124 hours.

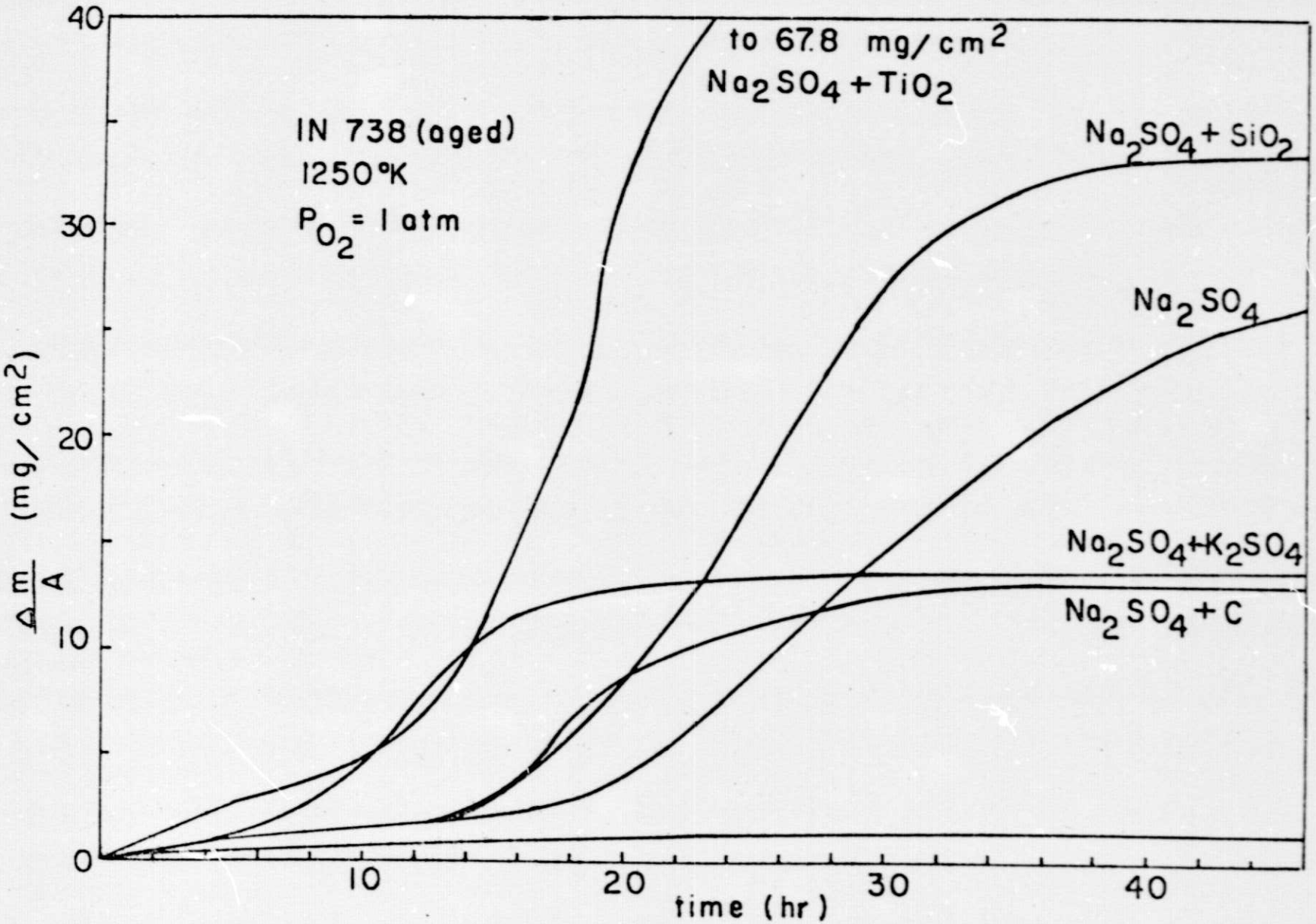

Figure 19 Weight Change vs Time for IN-738 Coated with 1 mg/cm² Salt in 1 atm O_2 at 977°C.

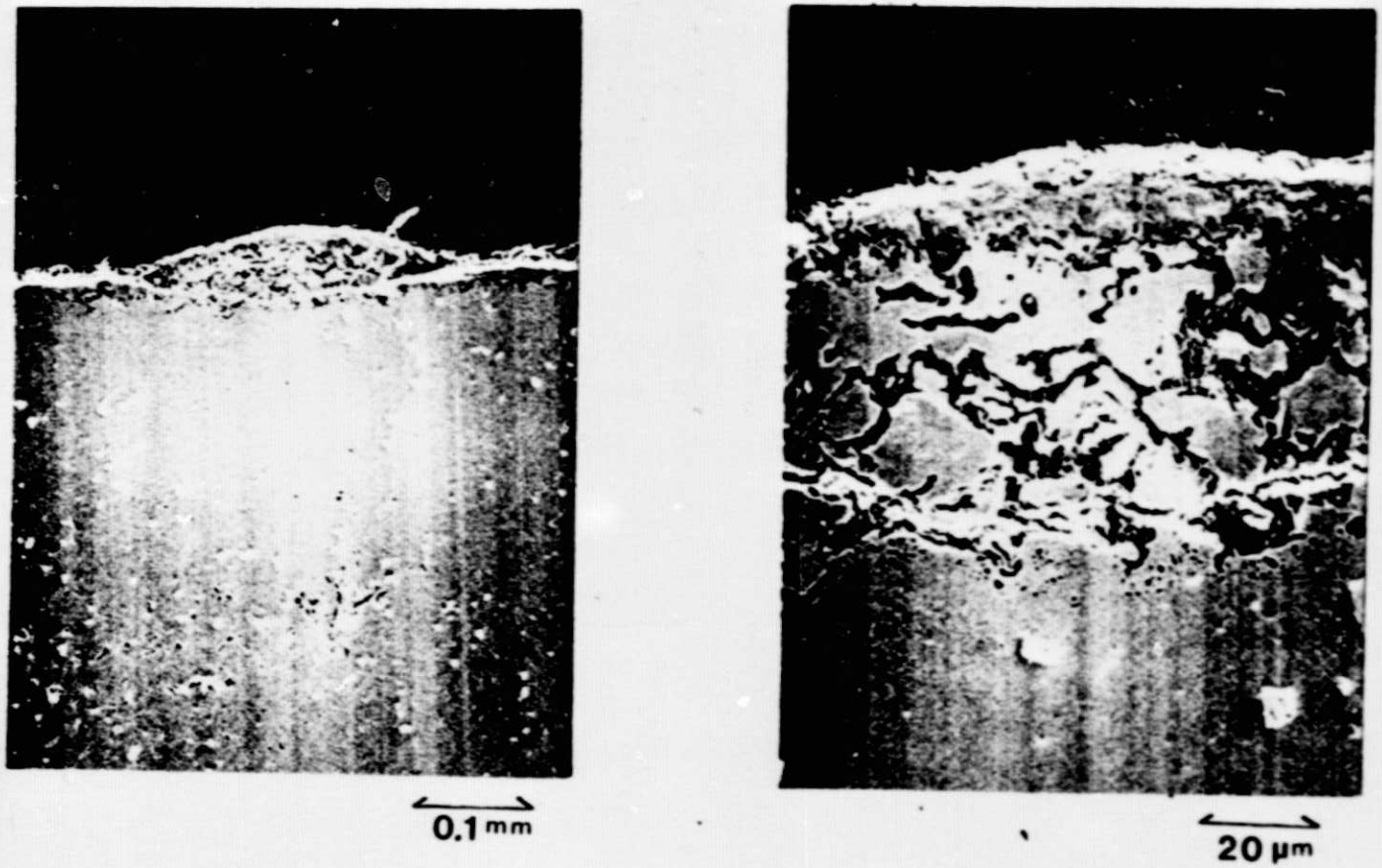

Figure 20 IN-738 Coated with 1 mg/cm^2 Na_2SO_4 + K_2SO_4 and Reacted for 8 hr at 977°C in 1 atm O_2.

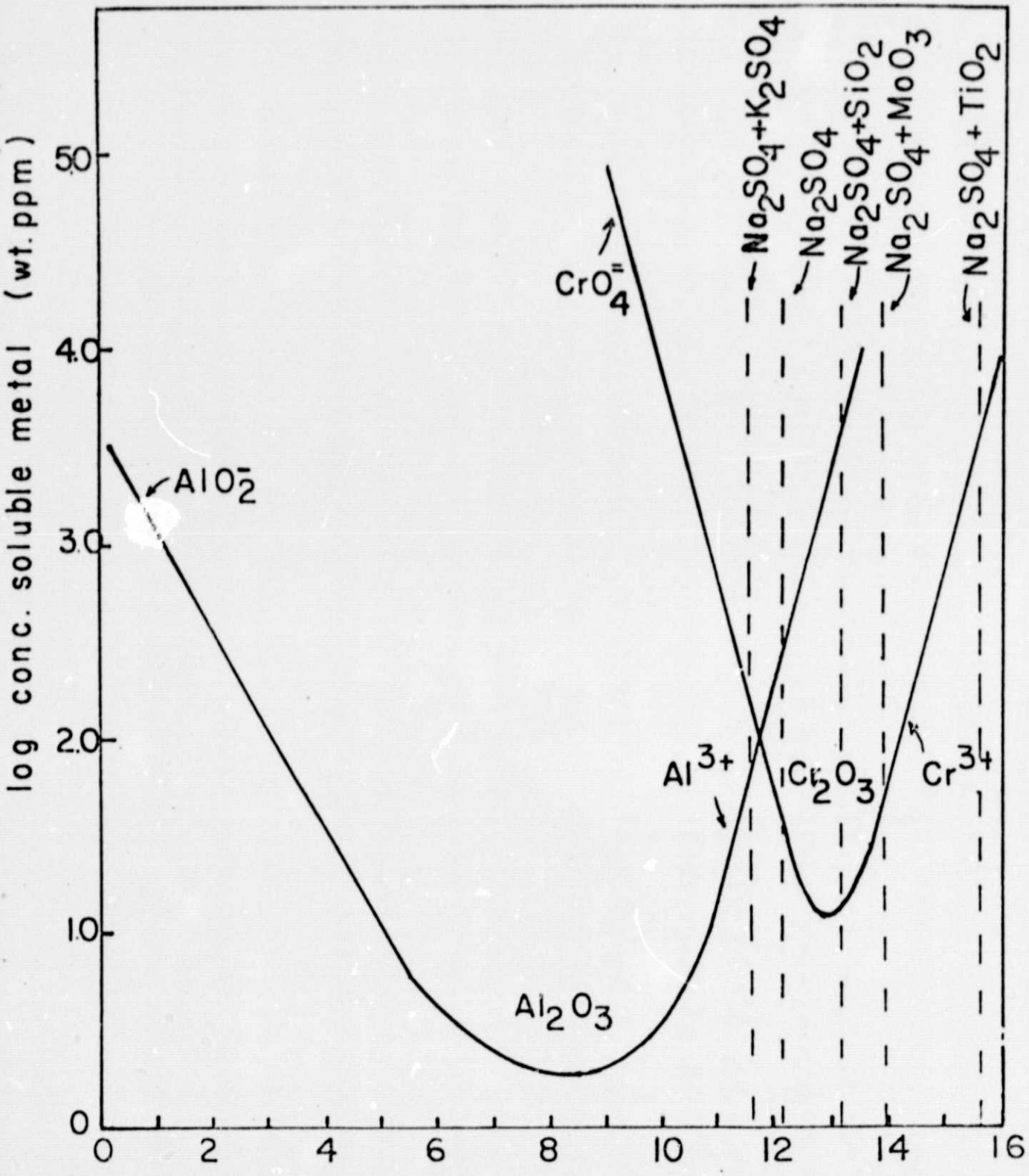

Figure 21 Solubilities for Al_2O_3 and Cr_2O_3 in Na_2SO_4 as Function of a_{Na_2O} for p_{O_2} = 1 atm, from work of Stroud and Rapp, (Ref. 27).

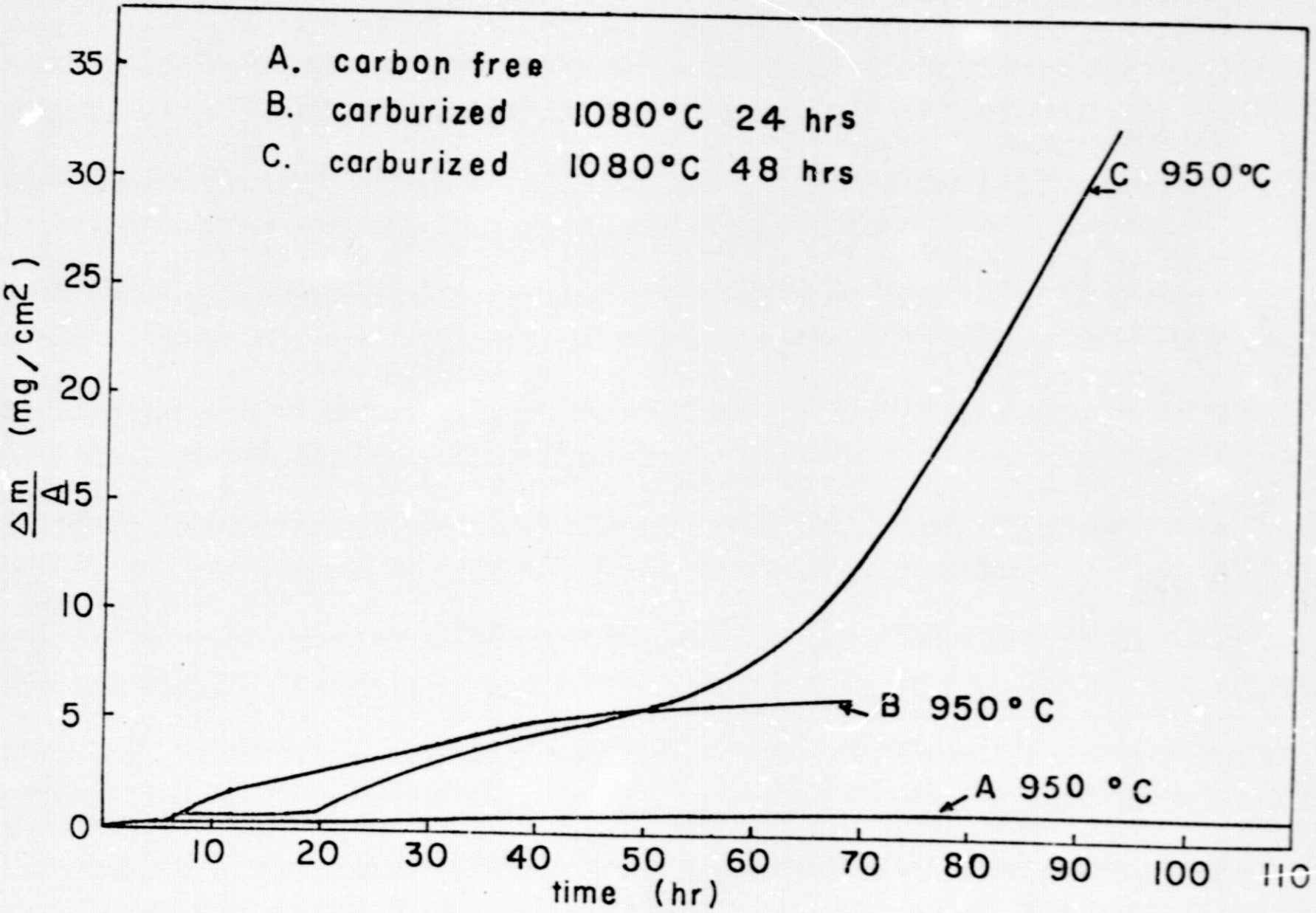

Figure 22 Weight Change vs Time for Ni-16Cr-3.4Al-3.4Ti-1.7Mo-2.6W-1.7Ta Coated with 1 mg/cm^2 Na_2SO_4 in 1 atm O_2.

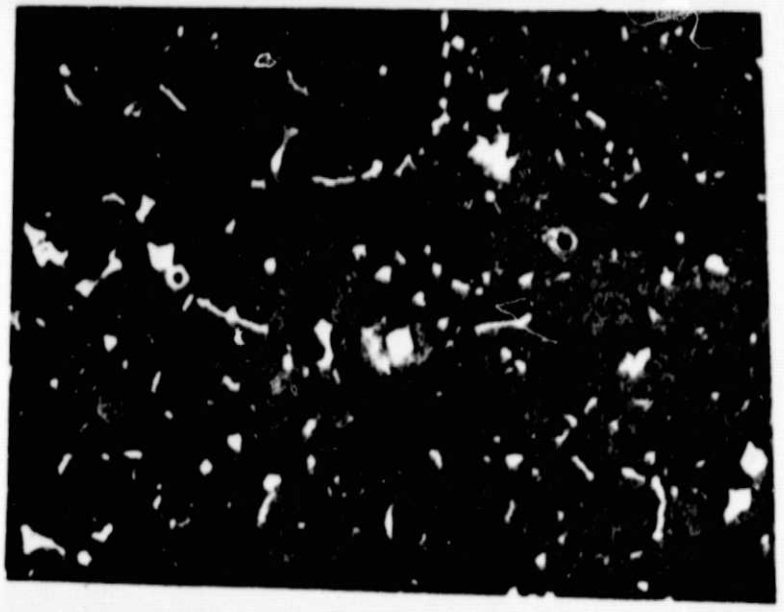

(a)
c#13
x1600

(b)
c#14
x1600

Figure 23 (a) Microstructure of alloy c#13, (b) Microstructure of alloy c#14.

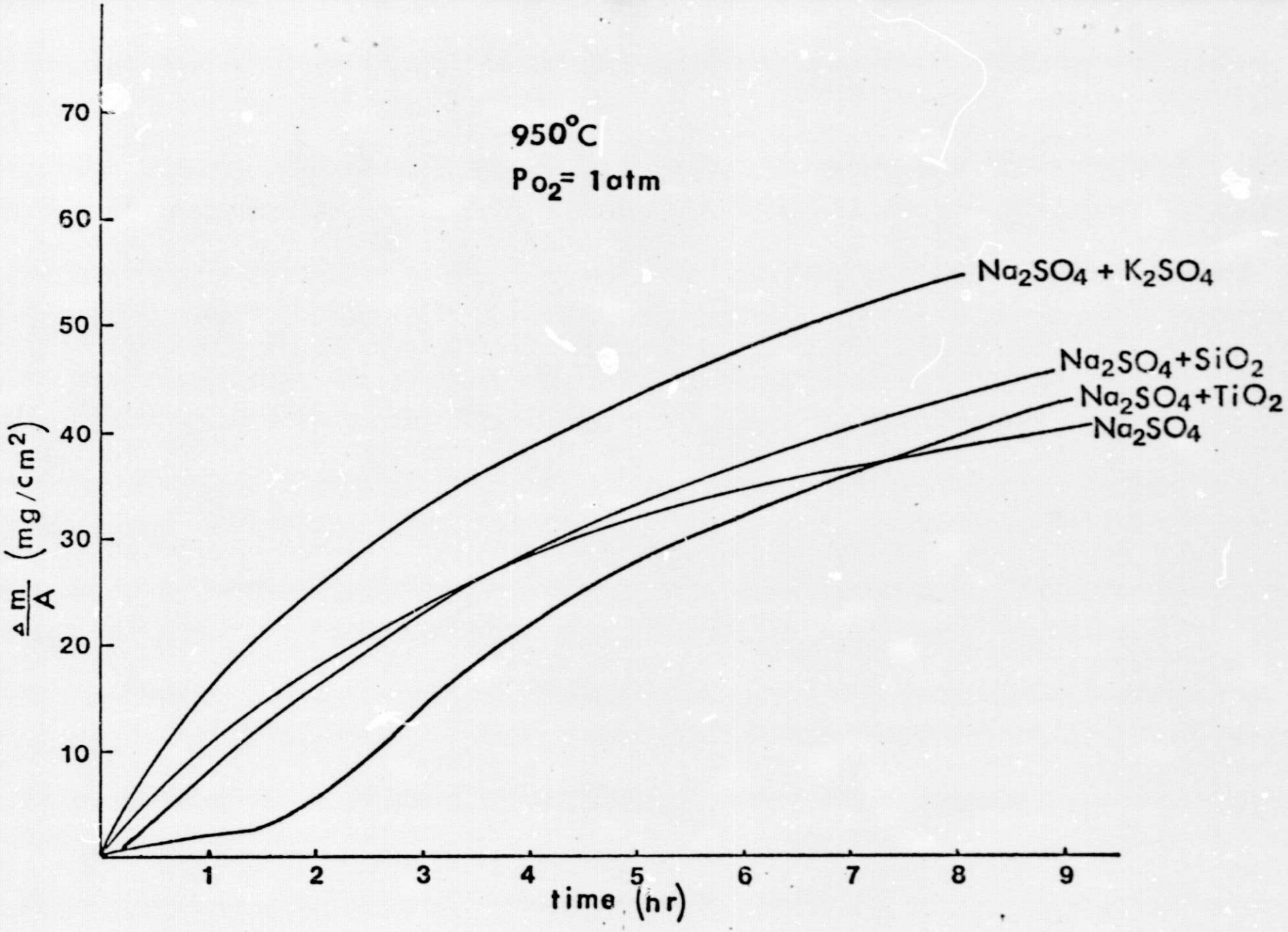

Figure 24 Weight Change vs Time for B-1900 coated with 1 mg/cm Salt in 1 atm O_2 at 950°C.

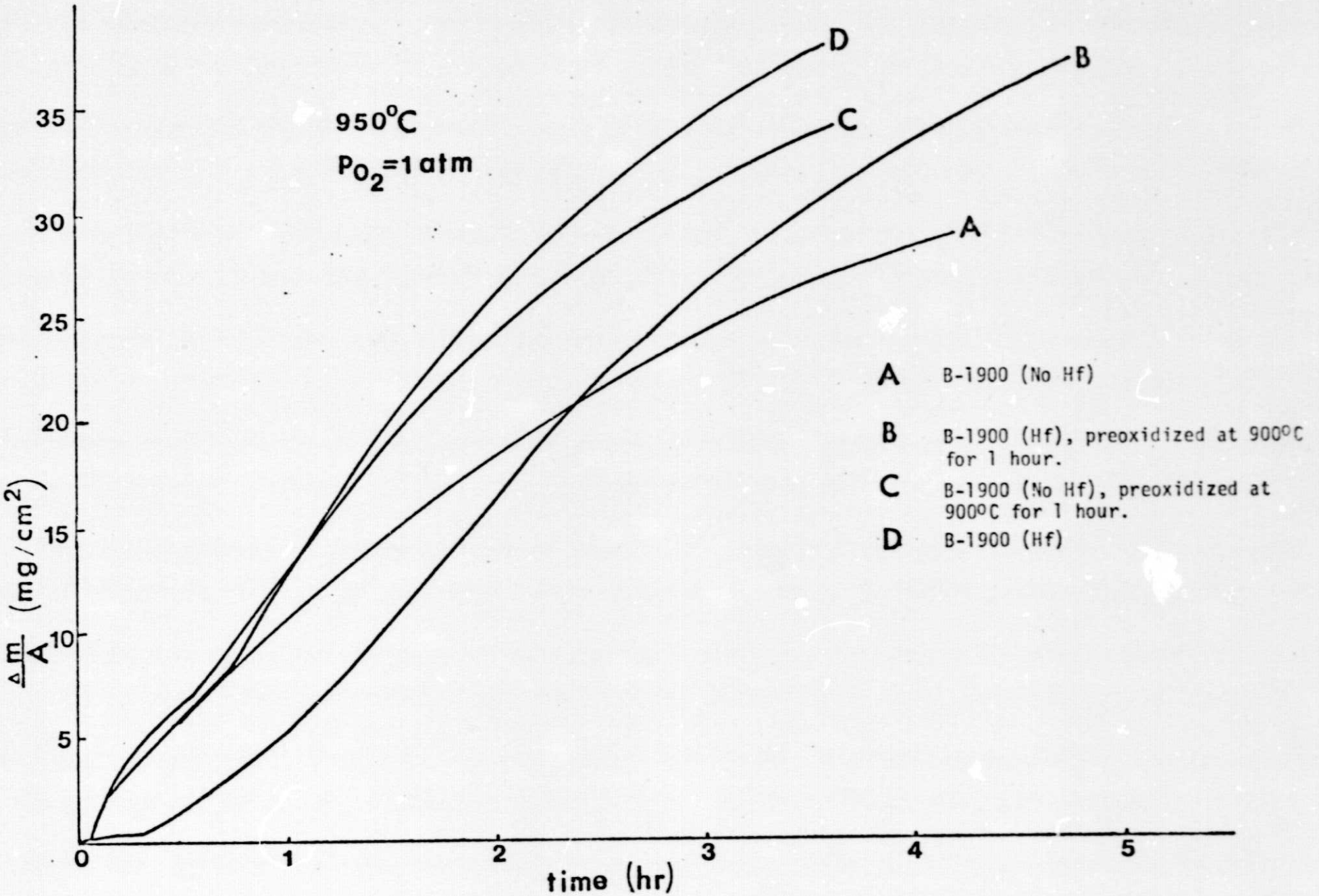

Figure 25 Weight Change vs Time of B-1900 (No Hf) and B-1900 (Hf) Oxidized at 950°C.

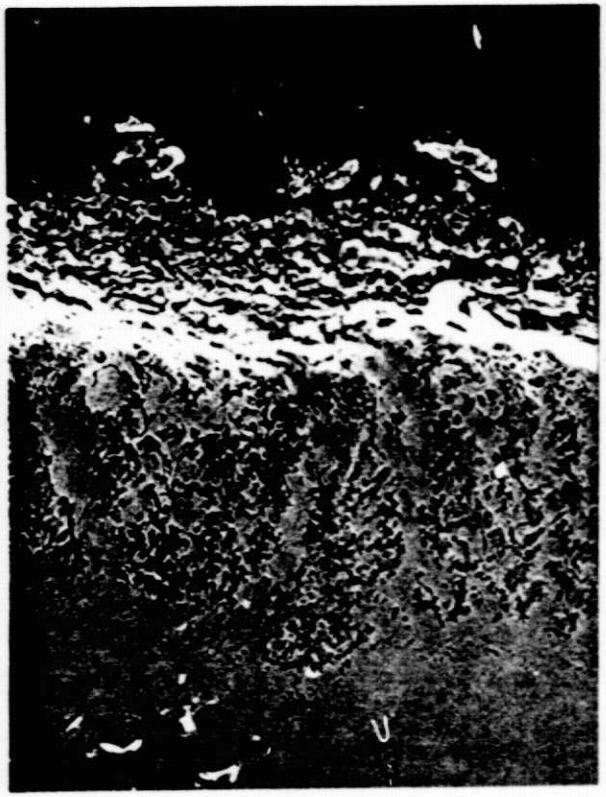

(a)
x800

(b)
x800

Figure 26 B-1900 coated with Na_2SO_4, oxidized at 950°C for 10 hours.